EGTRIB Journal
JOURNAL OF
THE EGYPTIAN SOCIETY OF TRIBOLOGY
VOLUME 21, No. 1, January 2024, pp. 62 - 77 **ISSN 2090 - 5882**
(Received September 21. 2023, Accepted in final form November 29. 2023) **jest.journals.ekb.eg**

ECO-GREEN SILVER NANOPARTICLES PREPARATION, CHARACTERIZATION, AND TRIBOLOGICAL ENHANCEMENTS ON 6061AMC

Gassour H.[1], Abu El-Magd G. A.[2], Mazen A.[2], Ibrahim A. M.[2]

[1]Mechanical Engineering Department, Higher Technological Institute at 10th of Ramadan city, 44629, EGYPT.
[2]Production Engineering and Mechanical Design department, Faculty of Engineering, Minia University 61519, EGYPT.

ABSTRACT
Nowadays, researchers are mostly drawn to green synthesis methods for nanoparticles because of their economic viability and environmental friendliness. Compared to the eco-green approaches developed in this work, traditional synthesis methods have one significant drawback: an extended reaction time.

This work presents a novel method for producing silver nanoparticles (AgNPs), which is then used to reinforce Al6061 alloy matrix. For a novel microwave assisted green AgNPs synthesis optimization, many trials have been made to speed up the reaction time. The approach involves microwave-irradiating extracts of Aloe vera leaves. The produced nanoparticles were used to investigate tribological characteristics of the reinforced Al6061matrix composition.

XRD analysis demonstrated improvements in particle sizes, particularly when utilizing the microwave-assisted approach, and confirmed the creation of AgNPs in the newly introduced green method. Indexing, inter atomic spacing, and specific surface area, were analyzed. Three samples, 0, 1, and 2 wt. % AgNPs contents, were manufactured using powder metallurgical technique for the purpose of investigating tribological enhancements. A dry wear test was performed monitoring many test parameters such as temperature, friction force, and humidity. The coefficient of friction (COF) and weight loss rates were evaluated in relation to the tribological properties. At different sliding speeds, the relationship between weight loss rates and AgNPs contents was examined, and substantial improved behavior was perceived.

KEYWORDS
Silver nanoparticles, tribological properties, aluminum matrix composites.

INTRODUCTION
Noble metal nanoparticles, like silver, have shown distinctly different physical, chemical, and biological characteristics from their bulk counterparts over the last few decades. Many researchers recently are concerned with characterization, synthesis, and silver nanoparticles' bio-applications, with a focus on antimicrobial activity as

well as engineering utilizations [1]. Nano silver particles (AgNPs) have a growing divers' applications in many sectors. Fig. 1 shows the common fields of applications. Recent research discussed the merits of using NPs in the industrial sector as a reinforcement to AMC and MMC.

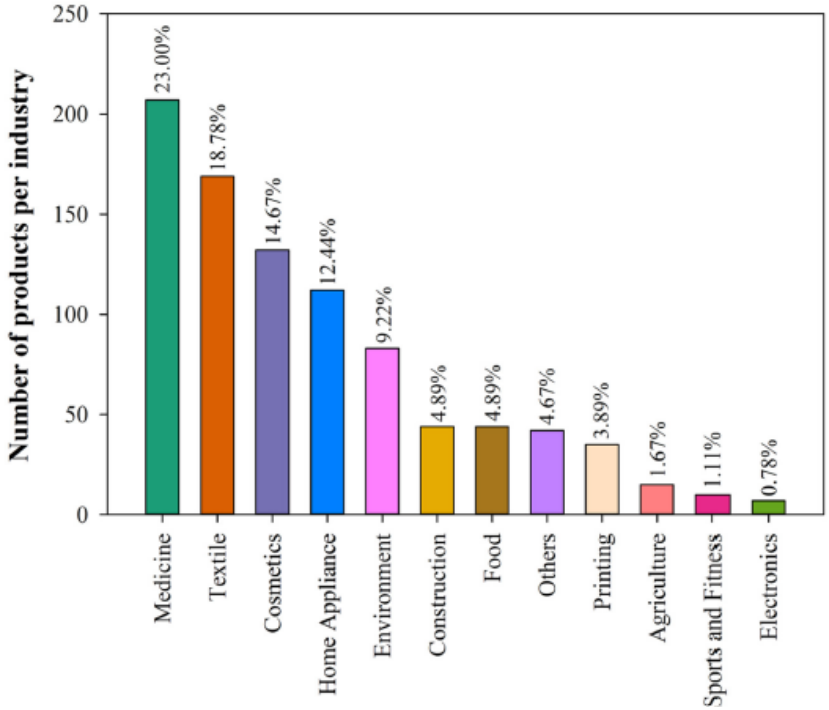

Fig. 1 Applications of AgNPs, [2].

Many recent reports aimed to present a comprehensive assessment of the global market focusing on historical data, industry-validated market data and projections with a suitable set of assumptions and methodology, [3]. Figure 2 shows the promising projections of nano silver market in the next few years, while it also shows the worldwide spread distribution among continents.

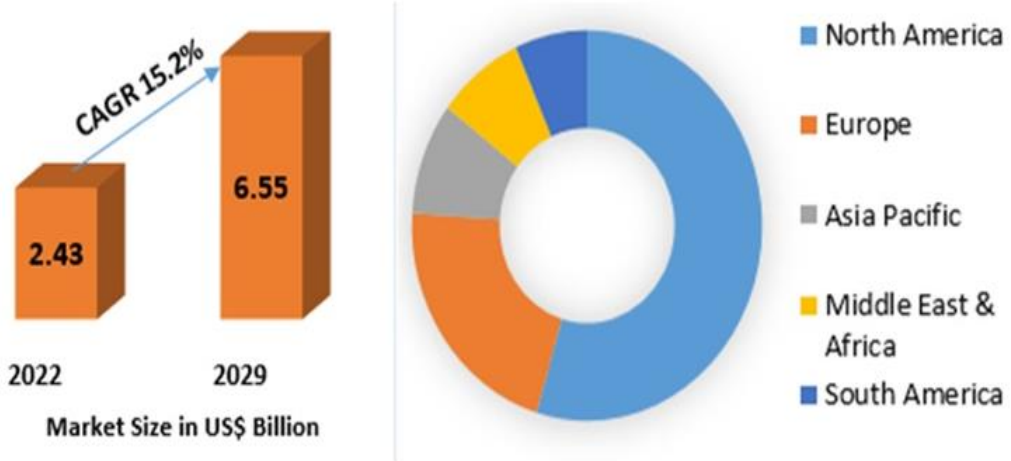

Fig. 2 Nano silver market and regional analysis, [3].

Utilizing green chemistry is being used for creating nanoparticles of silver. There are several ways to make silver nanoparticles, one of which is using plant extracts as fillers or reducers. The present research investigates a microwave assisted technique

for producing silver nanoparticles and using them to reinforce AMC for tribological improvements assessments. Ahmad and others, in 2003, published the first report on the extracellular synthesis of silver nano particles using eukaryotic systems, like fungi. They demonstrated that the reduction process is carried out by secreted enzymes, [4].

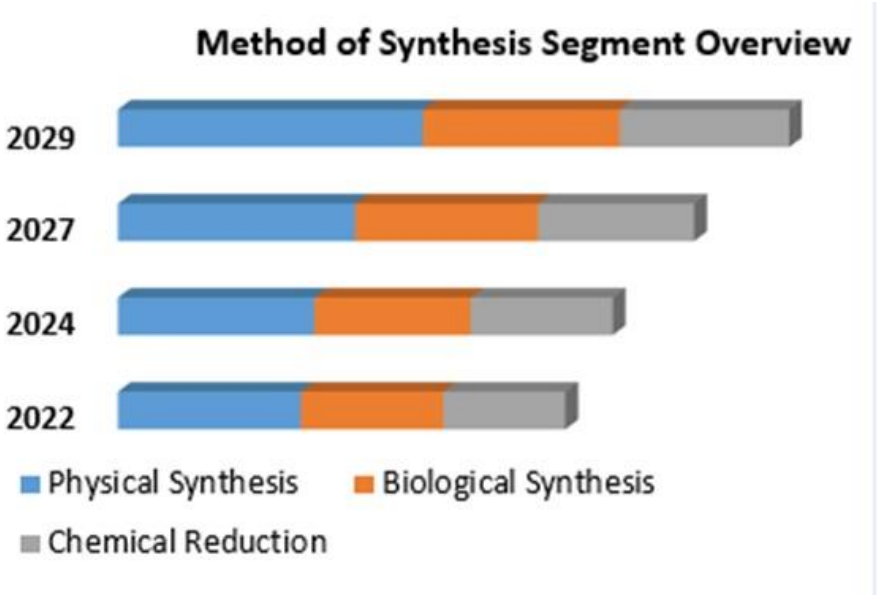

Fig. 3 Methods of Nano particles synthesis, [3].

Green synthesis with plants seems to be faster than synthesis with bacteria and fungi, and initial studies show that synthesis processes can generate AgNPs quickly. According to Shankar et al., utilizing geranium leaf yields a 90 % reaction in about nine hours as opposed to the 24 to 124 hours required for other reactions that have previously been reported, [5]. In 2014, Iravani and others studied the versatility of silver nanoparticle synthesis techniques and the ease with which silver NPs can be incorporated into various media. With the use of various synthetic techniques or by modifying the reaction conditions, such as the stabilizer or reducing agent, the shape, size, and size distribution of silver nanoparticles was manipulated.

Natural reducing and stabilizing agents can be used to conveniently synthesize NPs using biosynthetic methods. The biosynthesis of metal and semiconductor nanoparticles using organisms has been proposed as a potential environmentally and financially friendly substitute for chemical and physical methods. Such eco-friendly methods can potentially be used in various sectors including medical applications, [6]. In 2021, Amica Panja and others reviewed silver nano particles characteristics and behaviors. They mentioned the characterization methods (Fig. 4) and the three methods to prepare AgNPs: chemically, physically, and biologically.

The merits of biological methods are environmentally friendly, non-toxic, and sustainable, they are the most widely used of the three. They concluded that AgNPs are a simple, safe, and effective treatment for a wide range of illnesses, [7].

In 2013, A.M. Al-Qutub and others investigated the wear and friction behavior of Al6061 alloy reinforced with carbon nano tubes. It was discovered that the composite surpassed the basic alloy in terms of wear rate and friction coefficient under mild

wear conditions. The composite showed a greater wear rate and friction coefficient under extreme wear conditions. Examining the worn surfaces showed that for both materials, abrasion was the main wear mechanism at lower loads and the basic alloy was found to exhibit dominant adhesion at higher loads, [8].

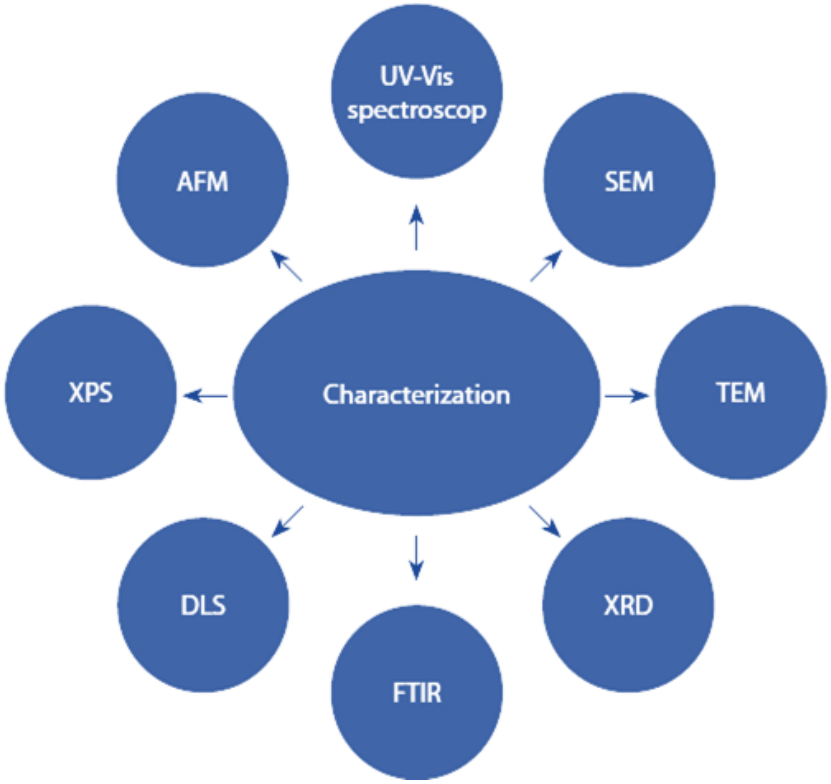

Fig. 4 Characterization methods of AgNPs.

They also gathered some green synthesis plants in Fig. 5. The prepared list contains the plant name and the used part of it.

Plant used	Part of plant
Pedalium murex	Leaf extract
White sugar	
Carpesium cernuum	Extract
Coriander sativum	Leaf extract
Salicornia brachiata	Aquoeus extract
Amaranthus gangeticus	Leaf extract
Ocimum sanctum (Tulsi)	Leaf extract
Parthenium	Slurry
Gum acacia	Gum
Red apple	Fruit extract
Coffea Arabica	Seed extract
Syzygium aromaticum	Bud extract
Putranjiva, drypetes roxburghii	Fruit extract
Lippia nodiflora	Aerial extract
Soymida febrifuga	Aqueous fruit extra

Fig. 5 Green synthesis plants, [7].

In 2019, Yulius Eka and others studied the engineering of aluminum matrix composite (AMC) reinforcement organoclay based on hot press method focusing on automotive industry. It is a commonly utilized material due to its notable mechanical strength, particularly when reinforced with nano-sized particles. XRD was used for characterization while the pressure used was 137 MPa, and temperature was varied from 490 °C – 600 °C with 3 hr. holding time. The hardness increased from 15 HVN to 197 HVN, while the mass density rises and reaches its maximum when 1 % by weight of organo-clay is added, [9].

In the same year, an attempt was made to study the behavior of aluminum alloy 7075 matrix reinforced with 0, 1, 3, and 5 weight percent Al_2O_3. Wear behavior and mechanical characteristics were investigated to determine the degree of improvements in hardness and tensile properties. A pin-on-disc device was used to study wear behavior to verify the increase in wear resistance. The outcomes demonstrated that the wear resistance and the mechanical properties were greatly improve, [10]. Later, Sanchez Lopez and others investigated silver effects on tribology and antibacterial properties. When compared to alumina, the tribological behavior did not clearly depend on the concentration of silver under lubricated or unlubricated conditions. The released Ag+ ion in the fluid media indicated that the bactericide behavior was improved by the dispersion of AgNPs. The fact that friction rubbing has no discernible effect on the released silver suggests that top segregation and diffusion are the most common mechanisms for its dissolution, [11].

In 2023, Anita and Aruna explored AgNPs hazards. They tracked the free silver ions that were released into the environment when materials containing big amounts of silver are used. These free silver ions build up in the atmosphere and eventually may cause harm to kidneys, liver, eyes, skin, and respiratory system, [12]. Dose-dependent nano silver-induced toxicity has also been investigated in certain instances. Smaller nanoparticles are more difficult for macrophages to eliminate from the body after inhalation, which eventually causes an accumulation of nano silver in the kidney, liver, lungs, and other organs. According to certain studies, nano silver can accumulate throughout one's lifetime. For that reason, small amounts of AgNPs were proposed for reinforcing AMC.

In general, as the reinforcement contents of AgNPs increases, the mechanical properties of the consolidated materials should be improved, [13]. In the current work, we examined two green synthesis approaches for AgNPs production, considering the previously mentioned facts. The first approach uses microwave radiation, and the second is a traditional green approach. After that, we reinforced Al6061-AMC with the extracted AgNPs and examined the wear rates and coefficients of friction behavior at various AgNPs addition contents and sliding speeds.

EXPERIMENTAL

Materials and Methods

Preparation of AgNPs

Local purchases were made of de-ionized water, ethanol, and Whatman filtration papers. Sliver nitrate $AgNO_3$ solution (1 mM) was purchased from Pub-chem. To get rid of any dirt, 50 grams of fresh aloe vera leaves were cut, cleaned, and then rinsed with deionized water several times. It was then chopped into tiny pieces and placed in a beaker filled with 50 milliliters of distilled water, boiling it for 20 minutes. After

that, it was allowed to reach room temperature before the extract was strained through filtration paper. Then, the Aloe vera water Extract (*AVWE*) was stored in refrigerator for later use (Fig. 6).

Figure 6 Aloe-Vera Extract (AVE) procedures.

Instead of using distilled water, ethanol was used to prepare Aloe vera ethanol extract (*AVEE*); it was treated according to the same used protocols and stored in the same environment. In a beaker with 50 ml of a 1 mM silver nitrate solution, AVWE (25 ml) was added dropwise and thoroughly mixed at room temperature. Then, the mixture was subjected to 90 sec microwave irradiations, every 10 min, using a domestic microwave oven that runs at 1250 W to reduce Ag+ ions. After 30 minutes, AVWE-AgNPs formation was fully established based on color change and later XRD analysis. The main indicator of the green synthesis process was the abrupt color shift from yellowish to blackish brown (Fig. 7).

Two-step centrifugations at 3000 rpm for 10 min each were used to collect the gray precipitate. Whatman paper was used for filtering, and de-ionized water was used for washing. The precipitate was then dried for 30 min at 60° C in dark environment. Using this approach, the obtained AgNPs were referred to as the First trial.

Fig. 7 Graphical demonstration of AgNPs formation.

The same steps were repeated, but this time using *AVEE* and the gray precipitates (AVEE-AgNPs) were gathered for additional examination and the trial was denoted as Second trial. As will be discussed later, XRD was used to characterize the produced nano-silver particles and revealed a diameter size range of13:64 nm. Particle size and shape, miller indices (h, k, l), D-spacing (the interplanar space between atoms), and specific surface area (SSA) were the features that were examined.

Test samples preparation

Al6061 powder preparation & Characterization

Metallurgical powder method was used to create the test samples. The Al6061 powder was obtained from Misr for Aluminum company, and it was refined using multi-stage sieves device. Nine distinct particle sizes, listed in Table 1, were obtained by screening Al6061 powder particles using the configuration depicted in Fig. 8, with sieves' mesh sizes ranging from 900 to 100 µm.

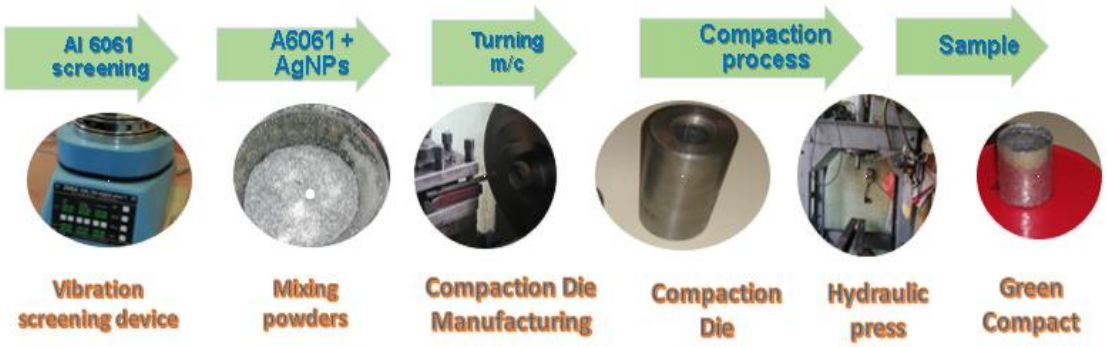

Fig. 8 Graphical demonstration for samples preparations.

Table 1 Aluminum powder particle sizes

sieve mesh no	1	2	3	4	5	6	7	8	9
Mesh size (micrometer)	900	800	700	600	500	400	300	200	100

The vibration pattern was chosen to speed up the screening procedure, which took 60 minutes at each run. After that, the powder was examined using Energy Dispersive Spectroscopy (EDS), which revealed the composition indicated in Table 2. The 100 µm-sized powder that was utilized to prepare the sample was cleaned, dried, and mixed with AgNPs at predefined percentages.

Table 2: Al6061 EDS results

Element wt.%	Al	Mg	Si	Cu	Fe
Spectrum	78.45	3.06	13.43	0.21	4.85

Samples Compaction & Sintering

To ensure adequate mixing of Al6061 powder with AgNPs at specified ratios of 1 wt.% and 2 wt.%, the mixing procedure was carried out using a milling machine with a rotation speed of 140 rpm for 30 min at each run. As illustrated in Fig. 8, the fabricated compaction die has dimensions of 10 mm for bore diameter and 50 mm for the length. Hydraulic press, 100-ton maximum capacity, was used for the compaction process. Several factors were considered in order to achieve good sample characteristics, including lubricant used, holding time, and compaction pressure.

Following several tests, the ideal settings were 600 MPa of pressure, 2 minutes of holding, and no lubricant. Pressure was manually adjusted to maintain a constant 600 MPa during the compaction holding time due to observed pressure declines while holding the press stationery that could be attributed to voids collapse.

The shape of the resulting green compact is displayed in Fig. 8. For optimization purposes, the sintering process was examined, and a three-zone tube furnace depicted in Fig. 9 was employed.

Fig. 9 Sintering -three Zone Furnace.

To minimize oxidation and prevent undesirable reactions, inert gas (N_2) was supplied to it. A dwell time of 120 minutes and a sintering temperature of 550° C were employed. Subsequently, chemical etching and polishing procedures were carried out in advance of wear test analysis.

Wear test

We conducted dry wear tests with a rotating pin-on-disc configuration. The temperature of the samples was continuously recorded during the tests to investigate any parameters related to temperature rise. Moreover, throughout the entire test run, the friction force was recorded. Fig. 10 shows a schematic diagram for the test configuration.

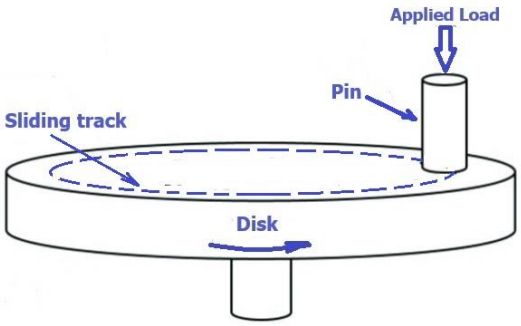

Fig. 10 Pin-on-disc configuration.

Figure 11 demonstrates the performed experimental work in a graphical representation.

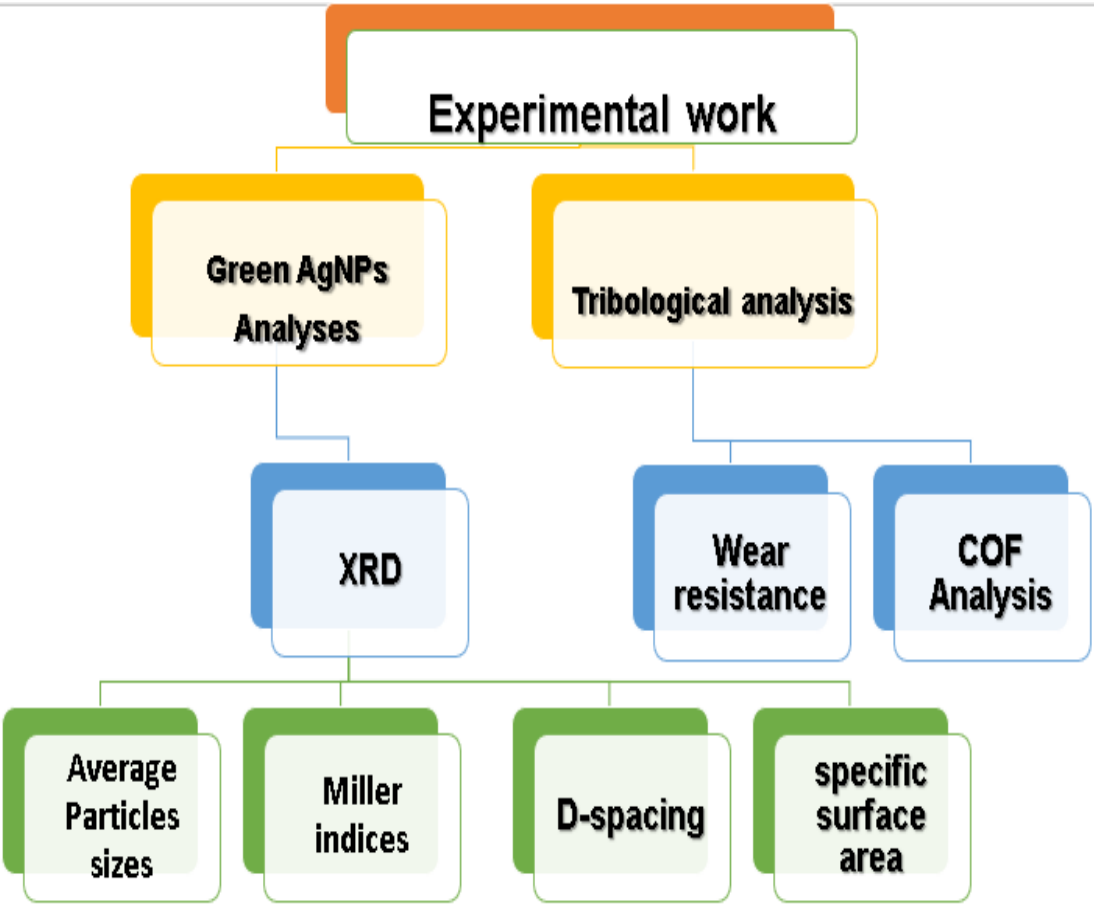

Fig. 11 Experimental work demonstration.

Green AgNPs Analyses

The produced amounts were subjected to XRD analysis to characterize the obtained silver nanoparticles (Fig. 12-A, B). The average crystallite diameters of each trial were then determined by processing the data. For that reason, analyses were conducted using Brunauer Emmet Teller's equation, Bragg's Law, and Scherrer's equation.

Average particles sizes

The first trial AgNPs were produced when *AVWE-$AgNO_3$* was exposed to microwave radiation, and XRD results are displayed in Fig. 12-A. The particles had an average diameter of 16 nm, placing them in the nano size range. Additionally, the Joint Committee on Powder Diffraction Standards JCPDS cards' values were used to assign the miller indices, [14]. Table 3 displays the information needed by Scherrer's equation to determine the average particle diameter's size.

The crystalline FCC structure of the generated nanoparticles, with an average size of 16.0105 nm, was also confirmed by calculations, [15]. The second trial XRD pattern was displayed in Figs. 12-B for produced AgNPs using AVEE-$AgNO_3$ mixture. The average particle's diameter is 24.096 nm and it also belonged to the nanosized range.

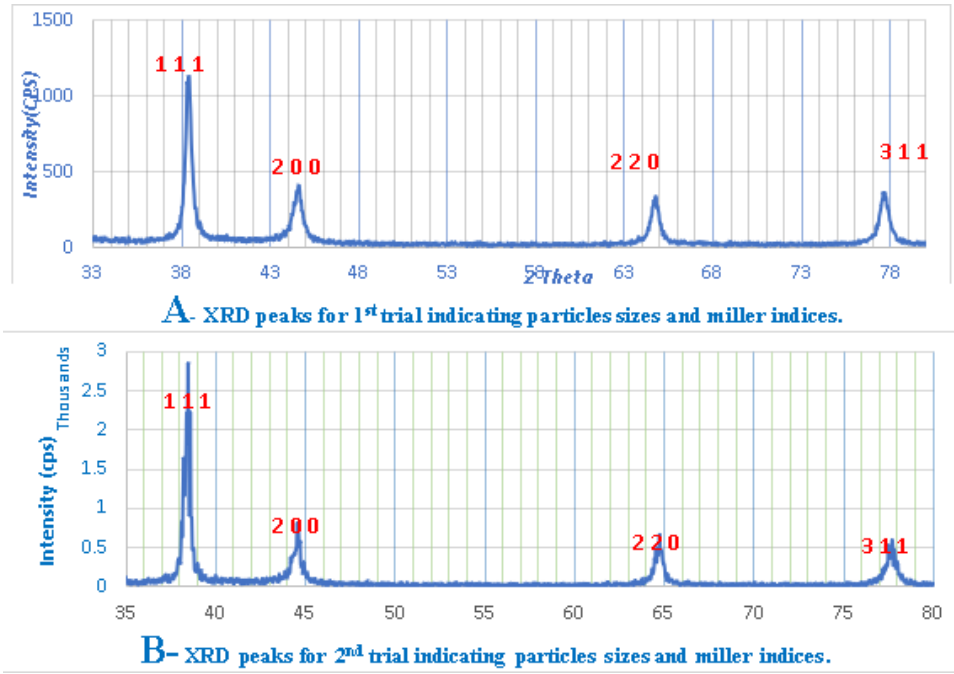

Fig. 12 XRD patterns for the synthesized AgNPs.

Table 3: XRD data of 1st extraction trial

	Pos [Deg]	JCPDS silver	Hight	Rate [CPS]	FWHM (Rad)	Miller indices h, k, l	Crystallite Size (nm)
Peak1	38.4	38.116	32.89	1127.08	0.007505	1 1 1	19.346
Peak2	44.6	44.277	19.87	411.46	0.011345	2 0 0	13.063
Peak3	64.76	64.426	18	337.5	0.010472	2 2 0	15.504
Peak4	77.6	77.472	18.73	365.63	0.010908	3 1 1	16.129

Table 4: XRD data of 2nd extraction trial

	Pos [deg]	JCPDS silver	Rate [CPS]	FWHM (Rad)	Miller indices (h,k,l)	Crystallite Size (nm)
Peak1	38.36	38.116	2225.983	0.006109	1 1 1	23.765
Peak2	44.52	44.277	815.10226	0.006632	2 0 0	22.339
Peak3	64.6	64.426	501.60528	0.010472	2 2 0	15.490
Peak4	77.68	77.472	607.06568	0.005061	3 1 1	34.779

Additionally, the analysis verified that the generated nanoparticles were FCC, which is defined as a non-primitive cell structure with an atomic packing factor (APF) of 0.74, [16]. Scherrer's equation (Eq. 1) was applied to calculate the average particle size:

$$D = \frac{K \times \lambda}{\beta \times \cos\theta} \qquad (1)$$

Where D is the particle size, K is Scherer's constant (K=0.94), λ is X-ray wavelength (0.154), β is the full width at half maximum (FWHM), θ is the angle of peak diffraction. Table 4 contained the extracted data from the XRD patterns that were used in crystallite size calculations for the second extraction trial.

Miller indices

The dimensions of the cell can be ascertained by peak positioning. This procedure, known as "indexing," is the first stage of XRD characterization and analysis. For comprehensive characterization, a Miller index (h, k, l) is typically assigned at each peak using the well-known Bragg's formula and the subsequent equation no.2:

$$d_{h\,k\,l} = \frac{a}{\sqrt{h^2+k^2+l^2}} \quad (2)$$

where: a (unit cell dimensions) $= 2r\sqrt{2}$, r = 0.144 nm (Atomic radius from the periodic table)

Table 5: First trial AgNPs indexing procedures at corresponding peaks.

Peak position 2θ	$(a/d)^2$	Approximated value	Reflection	Remarks
38.4	3.0189	3	(111)	$1^2+1^2+1^2=3$
44.6	4.0192	4	(200)	$2^2+0^2+0^2=4$
64.76	8.0055	8	(220)	$2^2+2^2+0^2=8$
77.6	10.9598	11	(311)	$3^2+1^2+1^2=11$

Table 5 lists the Indexing method and the needed data. All values were divided by 40 to determine a dividing constant that would allow the values in the second column to roughly become integers. The indices were then computed in accordance with published standards and displayed in the table.

Table 6: Second trial indexing data at corresponding peaks.

Peak position θ	$(a/d)^2$	Approximated value	Reflection	Remarks
19.18	3.012	3	(111)	$1^2+1^2+1^2=3$
22.26	4.005	4	(200)	$2^2+0^2+0^2=4$
32.3	7.970	8	(220)	$2^2+2^2+0^2=8$
38.84	10.978	11	(311)	$3^2+1^2+1^2=11$

To provide a thorough characterization for the second trial, Miller indices h, k, and l are also assigned at each peak. Table 6 lists the indexing method and the data that go with it. The indices were then computed in accordance with published standards and displayed in the table.

The D- spacing

The D-value (interplanar space between atoms) was determined using Bragg's formula (Eq. 3) as follows:

$$2 \,.\, d \,.\, \sin\theta = n \,.\, \lambda \quad (3)$$

where, λ is the wavelength of the X-ray beam (0.15418nm), (n=1). Then, the calculated D-spaces are listed in Table 7 and 8 for the first and second trials respectively.

Table 7: D-spacing data for 1st trial

Peaks (2θ)	h k l	θ (deg)	Particle size (nm)	D-spacing (nm)
38.4	1 1 1	19.2	19.346	0.234411
44.6	2 0 0	22.3	13.063	0.203159
64.76	2 2 0	32.3	15.504	0.143950
77.6	3 1 1	38.8	16.129	0.123028

Table 8: D-spacing data for the 2nd trial

Peaks (2θ)	h k l	θ (deg)	Particle size (nm)	D-spacing (nm)
38.36	1 1 1	19.18	23.765	0.2346463
44.52	2 0 0	22.26	22.339	0.2035056
64.6	2 2 0	32.3	15.490	0.1442681
77.68	3 1 1	38.84	34.779	0.1229215

Specific surface area (SSA)

Particle diameter, shape, and density are among the investigated parameters that have a reasonable relationship with specific surface area calculations (m^2/g). It was calculated using Brunauer Emmet Teller equation (Eq. 4) and found to be 36.281 m^2/gm and 24.316 m^2/gm for first and second trials respectively.

$$S = \frac{6\times10^3}{D_P\times\rho} \qquad (4)$$

Where D_p is the particle size, S is the specific surface area, and ρ is the silver density (10.5 g/cm^3).

It is evident from the earlier findings that the green synthesis of AgNPs through Aloe vera extraction is regarded as a significant substitute for conventional chemical reduction techniques. In addition to improving particle average sizes and many other properties, the microwave irradiations shortened the overall reduction time.

Tribological analysis

The following sections provide an overview of tribological characterization as reflected on the wear investigations that were conducted to highlight the benefits of utilizing the produced AgNPs to reinforce AMC 6061 as they relate to enhanced weight loss rate and improved coefficient of friction (COF).

Weight loss rate

Since weight loss rates primarily reflect material wear resistance, they were expressed in milligrams per meter (mg/m). Using a sensitive digital balance, the data is listed in Table 9. Each run's samples were weighed twice before and after.

Table 9: Weight loss rate at different conditions

AgNPs / Speed (m/s)	0%	1%	2%
0.2	0.112	0.092	0.035
0.4	0.025	0.011	0.024
0.6	0.014	0.013	0.023

The direct proportional relationship between sliding speed and wear resistance can be seen in Fig. 13. Simultaneously, it was found that the wear resistance pattern of the sample was enhanced by increasing its nano contents. In comparison to the unreinforced sample, it displayed the lowest weight loss rate values at 1wt. % nano silver additions at all test speeds. Lower shearing resistance to the surface layer is assumed to be the main reason for such behavior, provided by possible formation of minor silver islands during sintering, [17] [18].

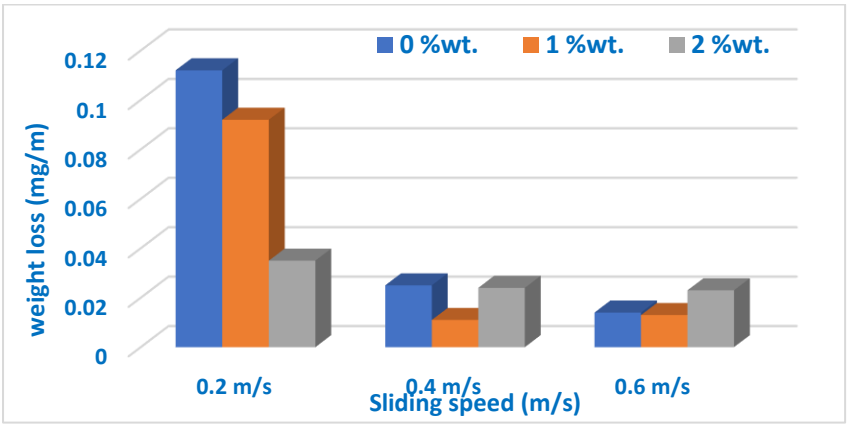

Fig. 13 Relation between weight loss rate and test sliding speed.

It is remarkable that at the lower sliding speed of 0.2 m/s, adding 1wt.% nano-silver increased the wear resistance by 18%, while adding 2 wt. % nano-silver improved it by 69% at the same speed. It is also obvious that higher sliding speeds acquired lower weight loss rates. Wear mechanism primarily tore rather than sheared the nano-silver particles, [19]. It has often been stated that by dispersing and coalescing across the surface, silver particles can prevent oxidation from occurring. As will be discussed later, a possible explanation for improving wear resistance is the increase in surface hardness caused by increased sliding speed that may lead to a slight increase in kinematic COF.

Coefficient of friction (COF)

The average COF behavior pattern at different reinforcement percentages and sliding speeds is shown in Fig. 14 while its corresponding data were listed in Table 10. As sliding speed increases, coefficients of friction generally rise as well. All reinforced samples exhibited higher COF at higher velocities relative to lower sliding speeds, disproving many earlier assertions and demonstrating the lack of a direct correlation between wear rates and COF.

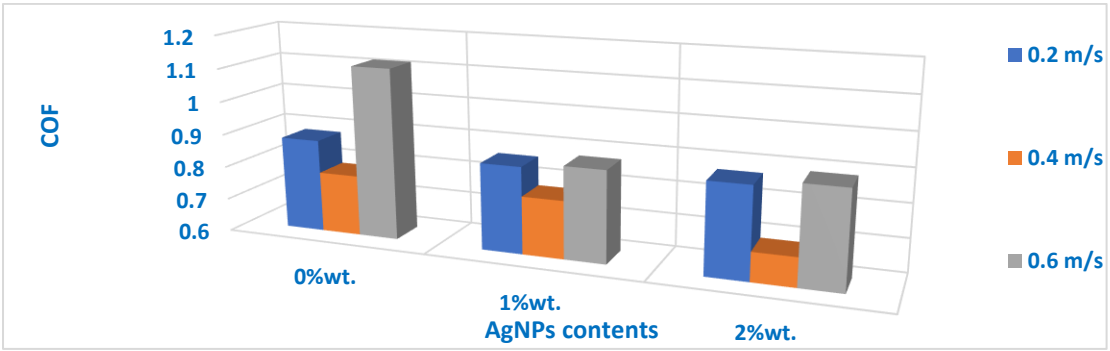

Fig. 14 Relation between average COF and reinforcement contents at varying sliding speeds.

Table 10 Average COF at different sliding speeds and reinforcement contents.

AgNPs wt.%	0.2 m/s	0.4 m/s	0.6 m/s
0	0.8809	0.7823	1.1163
1	0.8603	0.7733	0.8748
2	0.8721	0.6865	0.8893

From past discussions, the relationship between weight loss rates and the COF is believed to be inversely proportional. Many researchers investigated the effects of wettability on the coefficient of friction, [20], [21]. They studied its great effect on wear resistance, as lower wettability resulted in higher wear resistance, [22].

CONCLUSIONS

As demonstrated in the previous context, the green synthesis technique for producing silver nanoparticles has proven to be very important in introducing improved properties. Furthermore, the reduction process was enhanced, and the preparation time and particles' characteristics were improved by utilizing ethanol instead of water when using microwaves. Additionally, when using these particles to reinforce AMC, such a dispersion positively affected tribological properties and resulted in better wear resistance. The most noteworthy results are numerically summed up as follows:

1. The average AgNPs' size showed an improvement of 46.7% when using the microwave green-assisted method compared to the normal green method as it recorded 16 nm.

2. When employing AVE-2 without microwave irradiation, the interplanar space between atoms and the specific surface area (SSA) showed improvements of 6.5% and 22.7%, respectively, as it was averaged to 0.164948 nm and 18.796 m^2/gm.

3. There was a significant impact of reinforcement addition ratio on wear resistance. Remarkably, compared to unreinforced samples, it demonstrated a 69% improvement at a reinforcement ratio of 2 wt.% AgNPs at a modest sliding speed of 0.2 m/s.

4. When sliding speed is increased from 0.2 to 0.6 m/s, wear resistance also demonstrated improved behavior, reaching 85.7% and 67.4% at reinforcements of 0 wt.% and 1 wt.%, respectively.

5. The coefficient of friction decreased by 12.2% and 20.3%, respectively, at sliding speeds of 0.4 m/s and 0.6 m/s with AgNPs' reinforcement of 2 wt.%.

REFERENCES

1. Sunil T. G., Aditya S. H., Shradhey V. D., Omkar R. M., Pranav S. K., Supriya V. N., and Suresh G. K., "Silver Nanoparticles: Properties, Synthesis, Characterization, Applications and Future Trends", Intech Open, (2021).

2. Andrea L. H. and Sila T.S., "Understanding the potential environmental benefits of nano silver enabled consumer products", NanoImpact, Vol. 16, pp. 100285, (2019).

3. Ramesh A., Vikas G., and Raveena, "Nano silver Market – Global Industry Analysis and Forecast (2023-2029)," Maximize Market Research, Report ID 28828, (2023).

4. Protima R., Siim K., Stanislav F., and Erwan R., "A Review on the Green Synthesis of Silver Nanoparticles and Their Morphologies Studied via TEM", Advances in Materials Science and Engineering, Vol. 2015, ID 682749, (2015).

5. Shankar S. S., Ahmad A., and Sastry M., "Geranium leaf assisted biosynthesis of silver nanoparticles", Biotechnology Progress, Vol. 19, No. 6, pp. 1627–1631, (2003).

6. Iravani1 S., Korbekandi H., Mirmohammadi S.V., and Zolfaghari B., "Synthesis of silver nanoparticles: chemical, physical and biological methods", Research in Pharmaceutical Sciences, Vol. 9, No. 6, pp. 385-406, (2014).
7. Amica P., Ashish K. M., Mahesh D., Narendra K. P., Sachin K. S., and Bimlesh K., "Silver Nanoparticles – A Review", Eurasian Journal of Medicine and Oncology, Vol. 5, No. 2, pp. 95–102, (2021).
8. Al-Qutub A.M., Halil A., Saheb N., and Hakeem A.S., "Wear and friction behavior of Al6061 alloy reinforced with carbon nano tubes", Wear, Vol. 297, pp. 752–761, (2013).
9. Yulius E. A. and Bambang S., "Engineering of aluminum matrix composite (AMC) reinforcement organoclay based on hot press method using adaptive neuro-fuzzy inference system (ANFIS)", Materials Science and Engineering, Vol. 509, No. 012156, (2019).
10. Huda A. A., Adil A. M., and Hussain J. A., "Mechanical and wear behavior of AA7075 aluminum matrix composites reinforced by Al_2O_3 nanoparticles", Nanocomposites, Vol. 5, pp. 67–73, (2019).
11. Domínguez-Meister S., Rojas T.C., Frias J.E., and Sánchez-López J.C., "Silver effect on the tribological and antibacterial properties of a-C: Ag coatings", Tribology International, Vol. 140, pp. 105837, (2019).
12. Anita R. and Aruna S. P., "Re-exploring silver nanoparticles and its potential applications", Nanotechnology for Environmental Engineering, Vol. 8, pp. 789–804, (2023).
13. Gassour H., Gamal El-Din A. A. E. M., Asaad M., Ahmed M. M. I., "Characterization of aluminum composite reinforced by silver nanoparticles", Scientific reports, Vol. 13, No. 1, pp. 1-17 (2023).
14. Morris M. C., McMurdie H. F., Evans E. H., Paretzkin B., Parker H. S., Wong-Ng W., and Gladhill D. M., "Standard X-ray Diffraction Powder Patterns", Section 21 - Data for 92 Substances, L. O. Congress, Ed., U.S. department of commerce, Malcolm Baldrige, Secretary, (1985).
15. Lanje A. S., Sharma S. J., and Pode R. B., "Synthesis of silver nanoparticles: a safer alternative to conventional antimicrobial and antibacterial agents", Journal of Chemical and Pharmaceutical Research, Vol. 2, No. 3, pp. 478-483, (2010).
16. Istvan H. and Balazs H., "Science of Crystal Structures- Highlights in Crystallography", L. O. Congress, Ed., USA: Springer, pp. 333-334, (2015).
17. Ahmed M. M. I., Xiaoliang S., Wenzheng Z., and Kang Y., "Improving the tribological properties of NiAl matrix composites via hybrid lubricants of silver and graphene nano platelets", RSC Advances, Vol. 5, pp. 61554-61561, (2015).
18. Shorowordi K. M., Haseeb A. S. M. A., and Jean-Pierre C., "Velocity effects on the wear, friction and tribo-chemistry of aluminum MMC sliding against phenolic brake pad", Wear, Vol. 256, No. 11-12, pp. 1176-1181, (2004).
19. Hu J., Muratore, C., and Voevodin A., "Silver diffusion and high-temperature lubrication mechanisms of YSZ–Ag–Mo based nanocomposite coatings", Composites Science and Technology, Vol. 67, No. 3-4, pp. 336-347, (2007).
20. Adelina B., Gianni C., and Filippo M., "Influence of surface wettability on friction and wear tests," Wear, Vol. 222, pp. 57–65, (1998).
21. Chaoqun Z. and Masahiro F., "Influence of Wettability and Mechanical Properties on Tribological Performance of DLC Coatings under Water Lubrication", Journal of Surface Engineered Materials and Advanced Technology, Vol. 5, pp. 110-123, (2015).

22. Sarah C., Tom H., Sarah W., Susan C S., Amy K., and Anthony U., "Does surface wettability influence the friction and wear of large-diameter Co Cr Mo alloy hip resurfacings", J Engineering in Medicine, Vol. 227, No. 8, pp. 847–858, (2013).